ENCIT 2018

ABCM Associação Brasileira de Engenharia e Ciências Mecânicas

17th Brazilian Congress of Thermal Sciences and Engineering
November 25th-28th, 2018, Águas de Lindóia, SP, Brazil

ENCIT-2018-0426
STUDY OF AERODYNAMIC FLOWS USING UNSTRUCTURED GRIDS AND A CORRELATION-BASED TRANSITION MODEL

Leonardo Motta Maia de Oliveira Carvalho
Instituto Tecnológico de Aeronáutica, DCTA/ITA, 12228-904 - São José dos Campos - SP - Brazil
leonardo.mmoliva@gmail.com

Ricardo Galdino da Silva
João Luiz F. Azevedo
Instituto de Aeronáutica e Espaço, DCTA/IAE/ALA, 12228-904 - São José dos Campos - SP - Brazil
ri_galdino@yahoo.com.br, joaoluiz.azevedo@gmail.com

Abstract. *The present work is concerned with the study of the transitional flow phenomena over an airfoil subjected to high angle of attack and subsonic freestream conditions. The work is being conducted with an in-house CFD code which has transition prediction capabilities through the use of the $\gamma - Re_\theta$ transition model. The code solves the RANS equations in a fully coupled fashion with the turbulent and transition formulations. The results obtained for this configuration are presented and compared with experimental and numerical data available in the literature. Overall, the representation of this particular case is improved by the application of the transition model.*
Keywords: *CFD, Transition, Aerospace Applications, RANS Equations*

1. INTRODUCTION

It is well-known that laminar-to-turbulent flow transition can have dramatic effects in many aerospace applications. Therefore, an adequate handling of aerospace vehicle design has a need for accurate and robust techniques for transition prediction. Although high fidelity tools, such as Direct Numerical Simulations (DNS), are available to accurately predict transition at any condition, their computational cost is prohibitive to be applied to realistic flight configurations even for the most advanced research facilities today. Hence, simpler methodologies, such as empirical correlations and linear e^n methods (Langtry, 2006; Halila *et al.*, 2016) are used. However, these simplified methodologies suffer from the lack of accuracy when applied over more complex configurations. Furthermore, these simplified methodologies cannot always be organically integrated into the main aerodynamic tools used today in the industry, such as Computational Fluid Dynamics (CFD) codes (Johnson *et al.*, 2003; Menter *et al.*, 2006).

Modern CFD codes are state-of-the-art numerical tools that usually solve the Reynolds-averaged Navier-Stokes equations (RANS) coupled with complex turbulent closures (Bigarella and Azevedo, 2007). The solution of these equations is accomplished using sophisticated spatial discretization schemes and efficient time marching techniques. The calculations are also typically performed over unstructured grids that are distributed in many computational nodes, making extensive use of parallel architecture computers. The complex computational architecture of modern CFD codes imposes difficulties when trying to access any variable that is non-local to a given control volume (Langtry, 2006). This lack of information locality becomes a problem when trying to predict transition. The well established theories for transition prediction are commonly based on boundary layer information generated by profile integration (Langtry, 2006). However, the boundary layers are generally being calculated over many cells that, in modern computational architectures, can be spread over different computational nodes.

An organic way to include transition modeling capabilities into modern CFD codes without complex and expensive algorithms would be to modify currently available turbulence closures. One of such promising approaches to transition modeling is based on the intermittency function and empirical correlations. Basically, intermittency is defined as the period in which a given flow is laminar or turbulent. In transition modeling, the intermittency, γ, is used to limit the eddy viscosity coefficient or the production terms of turbulence models in laminar regions. In turbulent regions, however, the transition model restores the original behavior of the turbulence closure. This concept makes transition modeling modular as the goal of the transition formulation is, in essence, to clip the turbulence model in laminar flow regions. Among the models that are based on intermittency functions, the one presented in Langtry and Menter (2009) is, until now, one of the most successful models. It is also called $\gamma - Re_\theta$ transition model, and it uses four transport equations to account for transition effects. Two of these transport equations are those of the Shear-Stress Transport (SST) eddy viscosity closure (Menter, 1994). The other two equations deal with transition effects and are solved for intermittency and momentum

thickness Reynolds number, Re_θ.

The equations for γ and Re_θ are heavily based on empirical correlations. However, these correlations are available to the general public (Langtry and Menter, 2009; Rumsey, 2018) and they have already been extended to deal with different transition modes (Langtry *et al.*, 2015). Moreover, since these two extra equations can be solved separately from those of the SST closure, the transition model proposed in Langtry and Menter (2009) forms a flexible approach that can be coupled with different eddy viscosity models (Medida and Baeder, 2011) and recalibrated depending on the user needs. By being flexible and fully compatible with modern CFD codes, this transition prediction formulation is applied in the present work to study typical aerospace test cases.

2. THEORETICAL FORMULATION

2.1 Reynolds-Averaged Navier-Stokes Equations

In this work, the RANS equations are used to study transitional flows. The RANS equations can be written in Cartesian coordinates as

$$\frac{\partial \mathbf{Q}}{\partial t} + \nabla \cdot (\mathbf{E}_e - \mathbf{E}_v) = 0 \, . \tag{1}$$

Here, $\mathbf{Q}$, $\mathbf{E}_e$ and $\mathbf{E}_v$ are, respectively, the vector of conserved variables, the inviscid flux vector and viscous flux vector. These vectors can can be written as

$$\mathbf{Q} = \begin{Bmatrix} \rho \\ \rho u \\ \rho v \\ \rho w \\ e \end{Bmatrix} , \qquad \mathbf{E}_e = \begin{Bmatrix} \rho \mathbf{v} \\ \rho u \mathbf{v} + p\hat{i}_x \\ \rho v \mathbf{v} + p\hat{i}_y \\ \rho w \mathbf{v} + p\hat{i}_z \\ (e+p)\mathbf{v} \end{Bmatrix} , \qquad \mathbf{E}_v = \frac{1}{Re} \begin{Bmatrix} 0 \\ \left(\tau_{xj}^{\ell} + \tau_{xj}^{t}\right)\hat{i}_j \\ \left(\tau_{yj}^{\ell} + \tau_{yj}^{t}\right)\hat{i}_j \\ \left(\tau_{zj}^{\ell} + \tau_{zj}^{t}\right)\hat{i}_j \\ \beta_j \hat{i}_j \end{Bmatrix} . \tag{2}$$

The viscous stress tensor is defined as

$$\tau_{ij}^{\ell} \, = \, \mu_\ell \left[\left(\frac{\partial u_i}{\partial x_j} \, + \, \frac{\partial u_j}{\partial x_i} \right) \, - \, \frac{2}{3} \left(\frac{\partial u_m}{\partial x_m} \right) \delta_{ij} \right] \, , \tag{3}$$

and the components of the heat conduction vector can be written as

$$q_j \, = \, -\gamma \left(\frac{\mu_\ell}{Pr} \, + \, \frac{\mu_t}{Pr_t} \right) \frac{\partial (e_i)}{\partial x_j} \, . \tag{4}$$

In the previous equations, $\mathbf{v}$ is the velocity vector and τ_{ij}^{t} are the components of the turbulent stress tensor, which, for the closure considered in the present work, have an expression similar to that shown in Eq. (3), except that the eddy viscosity coefficient, μ_t, replaces the laminar dynamic viscosity coefficient, μ_ℓ.

2.2 Turbulence Closure

The $\gamma - Re_\theta$ transition model is coupled with the SST turbulent closure (Menter, 1994) in order to model the transition effects in the flowfield. Here, the transition formulation limits the production and destruction of turbulent kinetic energy, k. The SST turbulence closure equations can be written as

$$\begin{aligned} \frac{\partial (\rho k)}{\partial t} + \frac{\partial (\rho u_j k)}{\partial x_j} &= P_k - \beta^* \rho \omega k + \frac{\partial}{\partial x_j} \left[(\mu + \sigma_k \mu_t) \frac{\partial k}{\partial x_j} \right] \, , \\ \frac{\partial (\rho \omega)}{\partial t} + \frac{\partial (\rho u_j \omega)}{\partial x_j} &= \frac{\gamma}{\nu_t} P_k - \beta \rho \omega^2 + \frac{\partial}{\partial x_j} \left[(\mu + \sigma_\omega \mu_t) \frac{\partial \omega}{\partial x_j} \right] + 2(1 - F_1) \frac{\rho \sigma_{\omega 2}}{\omega} \frac{\partial k}{\partial x_j} \frac{\partial \omega}{\partial x_j} \, . \end{aligned} \tag{5}$$

In the above equations, P_k stands for the production term,

$$P_k = \tau_{ij} \frac{\partial u_i}{\partial x_j} \, , \qquad \tau_{ij} = \mu_t \left(2 S_{ij} - \frac{2}{3} \frac{\partial u_k}{\partial x_k} \delta_{ij} \right) - \frac{2}{3} \rho k \delta_{ij} \, , \qquad S_{ij} = \frac{1}{2} \left(\frac{\partial u_i}{\partial x_j} + \frac{\partial u_j}{\partial x_i} \right) \, . \tag{6}$$

Since the original SST closure combines the high Reynolds number Wilcox $k - \omega$ model (Wilcox, 1992) with the standard $k - \epsilon$ closure (Chien, 1982), a blending function is used to gradually switch between both model constants.

$$\phi = F_1 \phi_1 + (1 - F_1) \phi_2 \, . \tag{7}$$

In this expression, ϕ_1 is an arbitrary constant of the $k-\omega$ closure and ϕ_2 is a constant of the $k-\epsilon$ model. Moreover, the definitions needed to build the blending function, F_1, are:

$$F_1 = \tanh\left(\arg_1^4\right), \tag{8}$$

$$\arg_1 = \min\left[\max\left(\frac{\sqrt{k}}{\beta^*\omega d}, \frac{500\nu}{d^2\omega}\right), \frac{4\rho\sigma_{\omega 2}k}{\mathrm{CD}_{k\omega}d^2}\right], \tag{9}$$

$$\mathrm{CD}_{k\omega} = \max\left(2\rho\sigma_{\omega 2}\frac{1}{\omega}\frac{\partial k}{\partial x_j}\frac{\partial \omega}{\partial x_j}, 10^{-20}\right), \tag{10}$$

$$F_2 = \tanh\left(\arg_2^2\right), \tag{11}$$

$$\arg_2 = \max\left(2\frac{\sqrt{k}}{\beta^*\omega d}, \frac{500\nu}{d^2\omega}\right). \tag{12}$$

The differences between the implemented version of the model and the original definition, proposed on Menter (1994), are focused on the eddy viscosity coefficient definition, production limiter for turbulent kinetic energy and two of the model constants. Moreover, the eddy viscosity definition in the SST closure proposed in Menter *et al.* (2003) can be written as

$$\mu_t = \frac{\rho a_1 k}{\max(a_1\omega, SF_2)}, \qquad S = \sqrt{2S_{ij}S_{ij}}. \tag{13}$$

The production limiter of turbulent kinetic energy, k, is defined as

$$P_k = \min(P_k, 10\beta^*\rho\omega k). \tag{14}$$

The two constants modified in the updated version of the SST closure, γ_1 and γ_2, have their values re-defined as

$$\gamma_1 = 5/9; \qquad \gamma_2 = 0.44. \tag{15}$$

The other terms in Eq. (5), that are not explained in this section, are equivalent between both versions of the SST closure. These definitions can be found in Menter (1994); Menter *et al.* (2003).

2.3 Transition Modeling

The two additional transport equations solved by the $\gamma - Re_\theta$ model can be written as

$$\begin{aligned}
\frac{\partial(\rho\gamma)}{\partial t} + \frac{\partial(\rho u_j\gamma)}{\partial x_j} &= P_\gamma - E_\gamma + \frac{\partial}{\partial x_j}\left[\left(\mu + \frac{\mu_t}{\sigma_f}\right)\frac{\partial\gamma}{\partial x_j}\right] \\
\frac{\partial\left(\rho\hat{R}e_{\theta t}\right)}{\partial t} + \frac{\partial\left(\rho u_j\hat{R}e_{\theta t}\right)}{\partial x_j} &= P_{\theta t} + \frac{\partial}{\partial x_j}\left[\sigma_{\theta t}\left(\mu+\mu_t\right)\frac{\partial\hat{R}e_{\theta t}}{\partial x_j}\right].
\end{aligned} \tag{16}$$

These equations are solved for intermittency, γ, and transition momentum thickness Reynolds number, $\hat{R}e_\theta$. It avoids the need of non-local variables by correlating the strain rate Reynolds number, Re_v, with the momentum thickness Reynolds, Re_θ. This assumption allied with empirical correlations, that are based on experimental and numerical experiments, creates a very interesting and flexible procedure to model transitional flows.

3. NUMERICAL FORMULATION

The coupled system of partial differential equations formed by the RANS, turbulent and transition transport equations do not present a closed analytical solution. Moreover, to extract a valid solution from this system of partial differential equations, advanced numerical techniques are used. This section aims to briefly discuss these techniques.

3.1 Finite Volume Discretization

The RANS and turbulence model equations are discretized using a cell-centered finite volume method (Jameson and Mavriplis, 1986; Bigarella and Azevedo, 2007). The spatially discretized equations can be written as

$$\frac{\partial\mathbf{Q}_i}{\partial t} = -\frac{1}{V_i}\sum_{k=1}^{n_f}\left[\left(\mathbf{E}_{e_k} - \mathbf{E}_{v_k}\right)\cdot\mathbf{S}_k\right]. \tag{17}$$

Here, k indicates the number of the face, n_f is the total number of faces of the i-th control volume, and $\mathbf{S}_k$ is the area of the k-th face. For the convective flux computations, in order to include appropriate numerical dissipation, the Roe flux-difference splitting scheme (Roe, 1981) is used. Hence, the inviscid flux contribution for the k-th face can be written as

$$\mathbf{E}_{e_k} \cdot \mathbf{S}_k \;=\; \mathbf{E}_e\left(\mathbf{Q}_k\right) \cdot \mathbf{S}_k \;-\; \frac{1}{2}\left|\tilde{\mathbf{A}}_k\right| \left|\mathbf{S}_k\right| \left(\mathbf{Q}_R \;-\; \mathbf{Q}_L\right) \;, \tag{18}$$

where $\mathbf{Q}_k \;=\; 0.5\;\left(\mathbf{Q}_R + \mathbf{Q}_L\right)$ and $\left|\tilde{\mathbf{A}}_k\right|$ is the Roe matrix, formed with the magnitude of the eigenvalues associated with the k-th face normal direction.

3.2 Time Integration

An implicit time-stepping scheme based on the symmetric Gauss-Seidel method is used in order to advance the solution in time. The implicit scheme, used here, is detailed in Bigarella and Azevedo (2009). Its general form, including boundary conditions, can be expressed as

$$\left[\frac{V_i}{\Delta t_i}\mathbf{I} + \sum_{k=1}^{n_f}\frac{\partial(\mathbf{E}_k \cdot \mathbf{S}_k)}{\partial \mathbf{Q}_i} \;+\; \sum_{K_{BC}}\frac{\partial(\mathbf{E}_k \cdot S_k)}{\partial \mathbf{Q}_{nb}}\mathbf{B}_{nb}\right]\Delta\mathbf{Q}_i \;=\; -\sum_{k=1}^{n_f}\mathbf{E}_k \cdot \mathbf{S}_k \;-\; \sum_{k_{int}}\frac{\partial(\mathbf{E}_k \cdot \mathbf{S}_k)}{\partial \mathbf{Q}_{nb}}\Delta\mathbf{Q}_{nb}\;. \tag{19}$$

More information about the time integration procedures that are being used in BRU3D code can be found in Mulas *et al.* (2002) and in Bigarella and Azevedo (2009) as well.

4. RESULTS AND DISCUSSION

4.1 *Aerospatiale-A* Airfoil

The flow over the *Aerospatiale-A* airfoil presents various viscous phenomena that can be greatly influenced by transition. Over the upper surface of the airfoil, a small laminar separation bubble (LSB) imposes free transition. This bubble re-attaches at $x/c = 0.12$ and the turbulent boundary layer continues until $x/c = 0.83$. Since the separation bubble is the main transition trigger on this airfoil, the accurate prediction of the bubble structure is key for accurately representing the flow over this geometry.

This airfoil was also studied used in Langtry and Menter (2009) as a verification case during the development of the $\gamma - Re_\theta$ transition model, and further studied in Halila *et al.* (2016); Halila (2014) using a commercial CFD code. Further definitions about the conditions used to study the subsonic flow around this airfoil are shown in Table 1.

Table 1: Condition used while studying the *Aerospatiale-A* airfoil.

M_∞	α	Re	c	c_l	c_d	Tu (%)	μ_t/μ
0.15	13.3 deg	2×10^6	1.0 m	1.562	0.0208	0.2	10

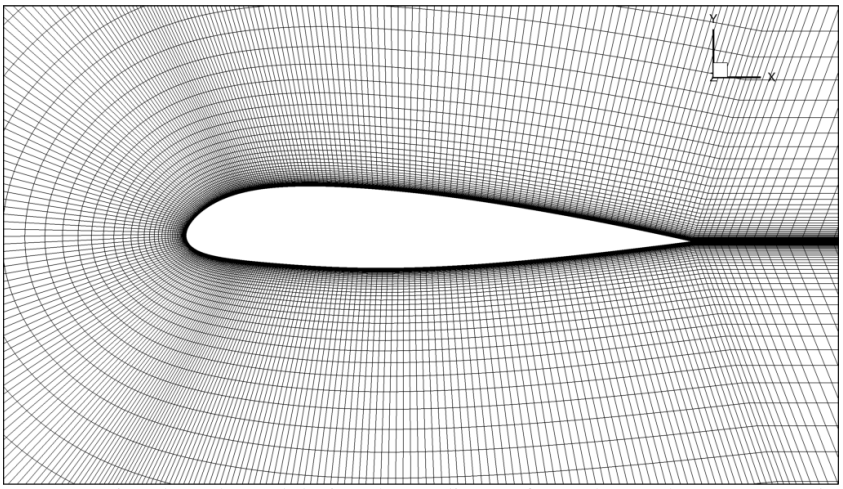

Figure 1: Computational mesh used during the studies performed over the *Aerospatiale-A* airfoil.

The mesh used during the studies is shown in Fig. 1. The grid is composed solely of hexahedral cells, which are extruded by one element in order to be used in BRU3D as a proper three dimensional mesh. As shown in Fig. 2, the y^+

values are kept close to 1 and the stretching used from the first volume is 5% for all cells along the airfoil chord. It is important to state that the mesh here considered can be considered perfectly adequate for any RANS turbulent calculation as it obeys all the rules commonly used in the industry to ensure a proper discretized domain for the turbulent closures to work.

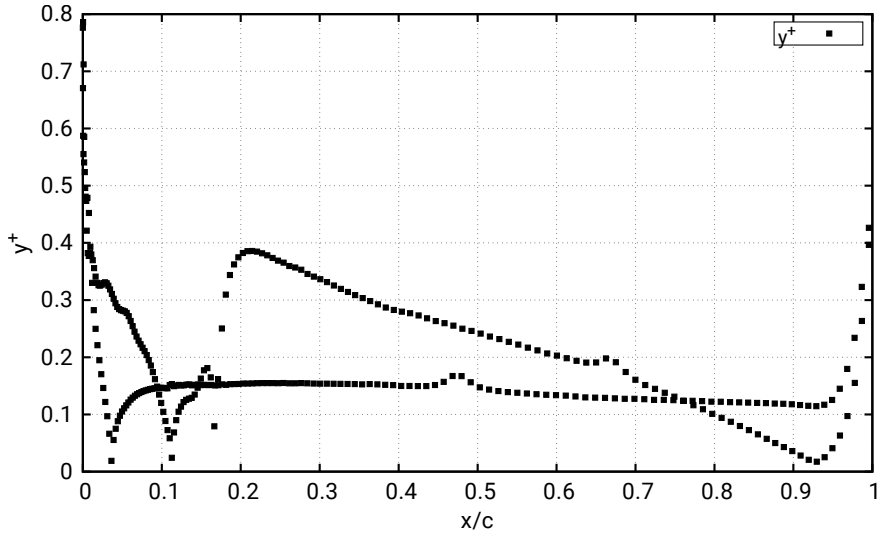

Figure 2: Distribution of y^+ over the *Aerospatiale-A* airfoil.

In Fig. 3, the pressure coefficient distribution over the *Aerospatiale-A* airfoil is shown. In the right upper side of Fig. 3, the peak suction region of the airfoil is highlighted. Overall, the agreement with the experimental data for both numerical solutions can be considered adequate. However, comparing both numerical solutions, it can be seen that the solution obtained with the $\gamma - Re_\theta$ transition model presents a higher peak suction coefficient while the SST solution falls lower than the experimental solution. Another perceivable difference is a slight peak in pressure coefficient obtained with the $\gamma - Re_\theta$ where the experiments indicate the LSB.

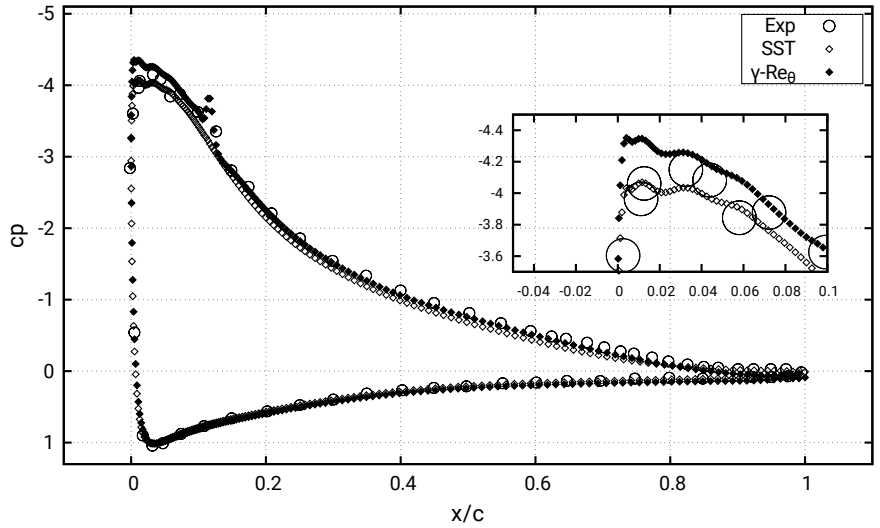

Figure 3: Pressure coefficient distributions over the *Aerospatiale-A* Airfoil.

In Fig. 4, the friction coefficient distribution over the *Aerospatiale-A* is shown. The solution obtained with the $\gamma - Re_\theta$ transition model and the SST turbulence closure are compared with the experimental data and the numerical results available in Ref. Halila *et al.* (2016). The behavior of the solution obtained with the SST closure greatly differs from the solution obtained with the $\gamma - Re_\theta$ transition model, completely ignoring the presence of the LSB. When compared with the experimental data, the solution obtained with the transition model appears to show better agreement. However, it is important to note that, based only on the experimental friction coefficient distributions, the identification of a transition region is not straightforward, as the more points are needed in order to sustain a solid conclusion regarding this phenomenon.

Another interesting observation that can be made based on Fig. 4, is actually related to pressure coefficient distributions

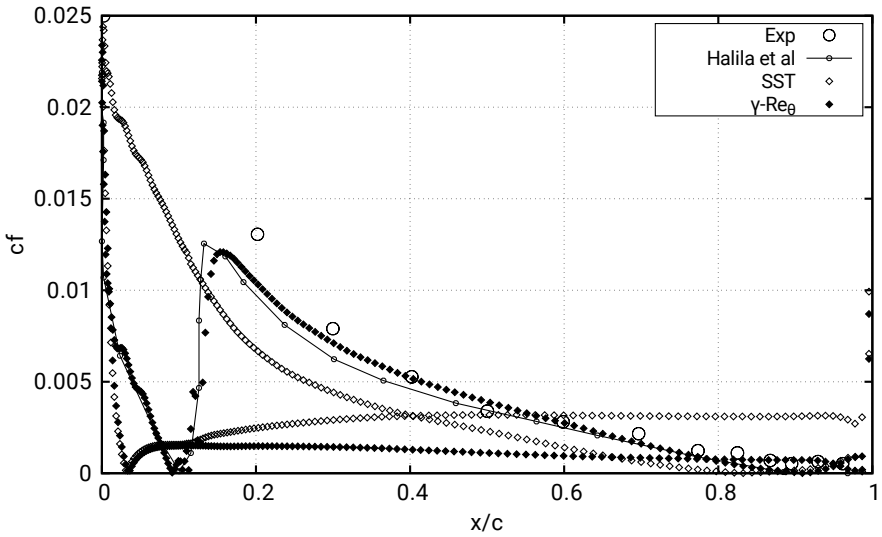

Figure 4: Friction coefficient distributions over the *Aerospatiale-A* airfoil.

shown in Fig. 3. As discussed, the peak suction pressure coefficient values observed in Fig. 3 are slightly different between the numerical solution obtained with the SST closure and the $\gamma - Re_\theta$ transition model. By observing the friction coefficient distributions, the differences in peak suction pressure coefficients can now be explained considering that the difference in friction coefficient is a strong indication that the boundary layer thickness of both solutions at that region is significantly different. Indeed, by observing the friction coefficient distributions shown in Fig. 4, it is seen that the numerical solution obtained with the $\gamma - Re_\theta$ transition model is indicating a laminar behavior, while the SST closure considers the whole flow turbulent.

Figure 5 shows the turbulence intensity contours over the *Aerospatiale-A* airfoil. Both solutions shows a production of turbulence in the stagnation point of the airfoil, what can be related to SST formulation. When comparing both contours over the lower surface of the airfoil, no significant difference is seen. However, at the upper surface, the SST closure shows higher turbulence intensity values close to the leading edge of the airfoil when compared to solution obtained with the $\gamma - Re_\theta$ transition model.

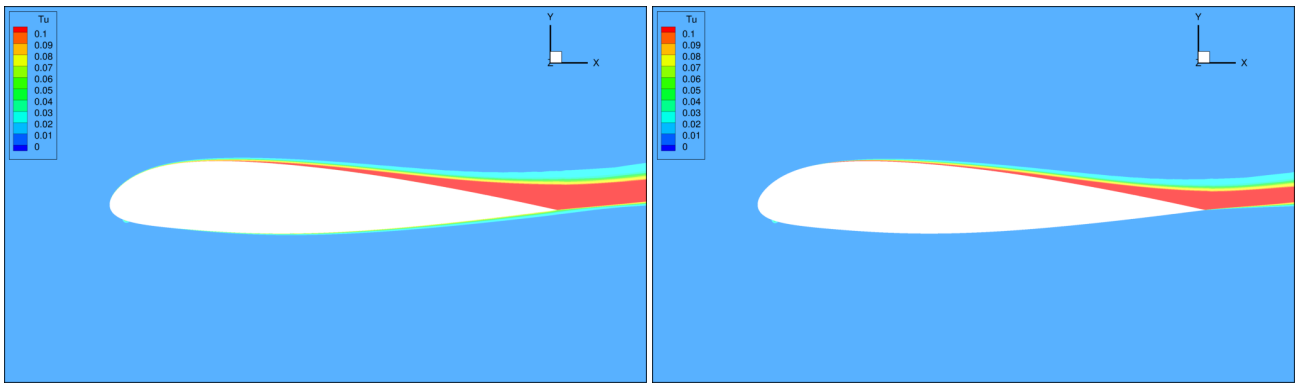

Figure 5: Turbulence intensity contours over the *Aerospatiale-A* airfoil. At the top, the contours obtained with the SST closure, and at the bottom, the contours obtained with the $\gamma - Re_\theta$ transition model.

Finally, in Fig. 6, the LSB, which is main transition trigger of this configuration, can be seen. Fig. 6a show the Mach number contours over the *Aerospatiale-A* airfoil. A classical subsonic flowfield is observed where regions of greater flow acceleration are associated with the regions where the airfoil is thicker. Moreover, Fig. 6a also highlights the the region where the LSB is expected.

Figure 6b and Fig. 6c show the velocity profiles at the region highlighted in Fig. 6a which are obtained, respectively, with the SST closure and the $\gamma - Re_\theta$ transition model. It is observed that the velocity profiles shown in Fig. 6b are all attached to the upper surface of the airfoil. However, the velocity profiles shown in Fig. 6c show a clear reversion in direction, indicating the existance of a laminar separation bubble.

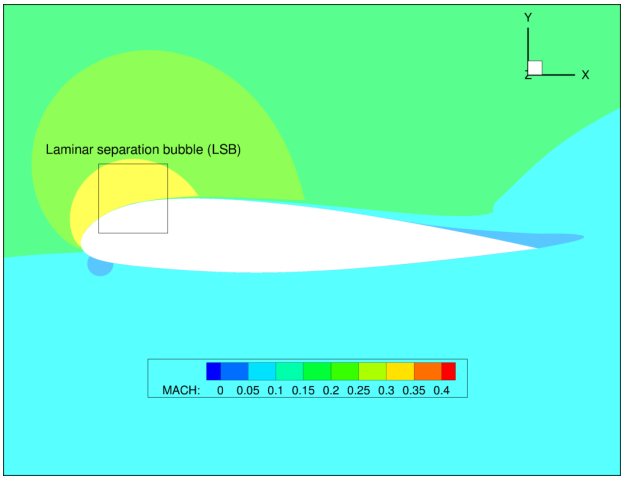

(a) Mach number contours.

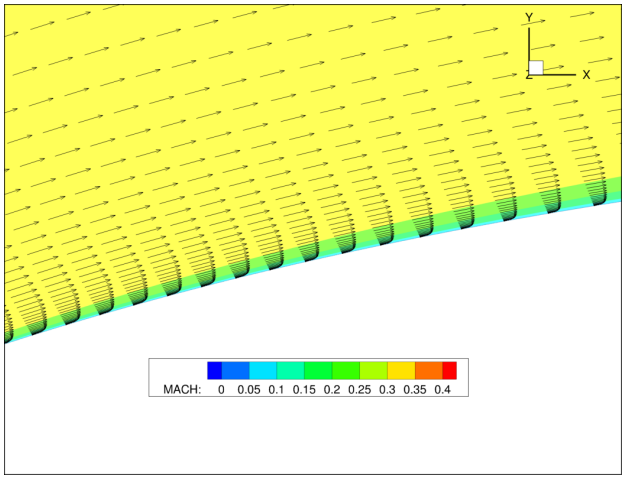

(b) SST closure.

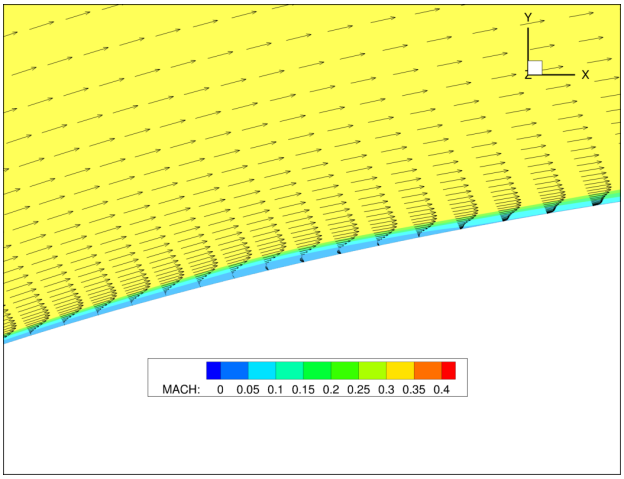

(c) $\gamma - Re_\theta$.

Figure 6: Details of the separation bubble over the *Aerospatiale-A* airfoil.

5. CONCLUDING REMARKS

The study of transitional flows is the main objective of the present contribution. This paper has briefly presented the theoretical and numerical formulations of a correlation-based transition model, which can be coupled to standard eddy-viscosity turbulence closures. In the particular case of the present contribution, it has been coupled to the SST turbulence model. The calculations performed have indicated that accurate results can be obtained with this capability when compared to the experimental and numerical data available in the literature.

The configuration addressed so far is the *Aerospatiale-A* airfoil, which has been studied for low subsonic flight conditions. It is interesting to see that the transition model is capable of capturing the laminar separation bubble near the leading edge of the airfoil, which triggers the flow transition. This effect can be seen clearly when comparing the friction coefficient distributions over the airfoil with the experimental data and other numerical results available in the literature.

By analyzing the contours of turbulence intensity, it is seen that the use of the SST closure alone leads to a significant increase in turbulence intensity over the upper surface of the airfoil, which can lead to greater values of drag over the configuration. More importantly, the Mach number contours and the analysis of the velocity profiles shows that, not only the turbulence intensity values are greater overall, but the laminar separation bubble, which is an important phenomenon associated with this configuration, is completely ignored by the SST closure.

In general, the application of the transition model to study the *Aerospatiale-A* airfoil proved to be essential, as the main transition triggers are completely ignored by the SST closure. However, the simplicity associated with the configuration and the reliable experimental and numerical data available in the literature, makes this case ideal to explore the possibilities related to transition models, which is not always trough in real world applications. In real world applications, where experimental data is sometimes not reliable or available, the use of the transition model shall be carefully considered since this type of empirical formulation is known to have great sensibility to mesh quality and numerical schemes.

6. ACKNOWLEDGMENTS

The authors gratefully acknowledge the support for the present research provided by Conselho Nacional de Desenvolvimento Científico e Tecnológico, CNPq, under the Research Grants No. 309985/2013-7, No. 400844/2014-1 and No. 443839/2014-0. The work is also supported by Fundação de Amparo à Pesquisa do Estado de São Paulo, FAPESP, under the Research Grant No. 2013/07375-0. The support provided by Conselho Nacional de Desenvolvimento Científico e Tecnológico, CNPq, through a graduate scholarship for the first author, is also greatly appreciated.

7. REFERENCES

Bigarella, E.D.V. and Azevedo, J.L.F., 2007. "Advanced eddy-viscosity and Reynolds-stress turbulence model simulations of aerospace applications". *AIAA Journal*, Vol. 45, No. 10, pp. 2369–2390.

Bigarella, E.D.V. and Azevedo, J.L.F., 2009. "A unified implicit CFD approach for turbulent-flow aerospace-configuration simulations". In *47th AIAA Aerospace Sciences Meeting Including The New Horizons Forum and Aerospace Exposition*. AIAA Paper No. 2009-1473, Orlando, FL.

Chien, K.Y., 1982. "Predictions of channel and boundary-layer flows with a low-Reynolds-number turbulence model". *AIAA Journal*, Vol. 20, No. 01, pp. 33–38.

Halila, G.L.O., 2014. *A Numerical Study on Transitional Flows by Means of a Correlation-Based Transition Model*. Master's thesis, Instituto Tecnológico de Aeronáutica, São José dos Campos, SP, Brazil.

Halila, G.L.O., Bigarella, E.D.V. and Azevedo, J.L.F., 2016. "Numerical study on transitional flows using a correlation-based transition model". *Journal of Aircraft*, Vol. 53, No. 4, pp. 922–941.

Jameson, A. and Mavriplis, D., 1986. "Finite-volume solution of the two-dimensional Euler equations on a regular triangular mesh". *AIAA Journal*, Vol. 24, No. 4, pp. 611–618.

Johnson, F.T., Tinoco, E.N. and Yu, N.J., 2003. "Thirty years of development and application of CFD at Boeing Commercial Airplanes, Seattle". In *16th AIAA Computational Fluid Dynamics Conference*. AIAA Paper No. 2003-3439, Orlando, FL.

Langtry, R.B., 2006. *A Correlation-Based Transition Model using Local Variables for Unstructured Parallelized CFD Codes*. Ph.D. Thesis, University of Stuttgart, Stuttgart, Germany.

Langtry, R.B. and Menter, F.R., 2009. "Correlation-based transition modeling for unstructured parallelized computational fluid dynamics codes". *AIAA Journal*, Vol. 47, No. 12, pp. 2894–2906.

Langtry, R.B., Sengupta, K., Yeh, D.T. and Dorgan, A.J., 2015. "Extending the $\gamma - Re_\theta$ local correlation based transition model for crossflow effects". In *45th AIAA Fluid Dynamics Conference*. AIAA Paper No. 2015-2474, Dallas, TX.

Medida, S. and Baeder, J.D., 2011. "Application of the correlation-based $\gamma - Re_{\theta t}$ transition model to the Spalart-Allmaras turbulence model". In *20th AIAA Computational Fluid Dynamics Conference*. AIAA Paper No. 2011-3979, Honolulu, HI.

Menter, F.R., 1994. "Two-equation eddy-viscosity turbulence models for engineering applications". *AIAA Journal*, Vol. 32, No. 8, pp. 1598–1605.

Menter, F.R., Langtry, R. and Volker, S., 2006. "Transition modelling for general purpose CFD codes". *Flow, Turbulence and Combustion*, Vol. 77, pp. 277–303.

Menter, F., Kuntz, M. and Langtry, R.B., 2003. "Ten years of industrial experience with the SST turbulence model". *Heat and Mass Transfer*, Vol. 4, pp. 625–632.

Mulas, M., Chibbaro, S., Delussu, G., Piazza, I.D. and Talisse, M., 2002. "Efficient parallel computations of flows of arbitrary fluids for all regimes of Reynolds". *International Journal of Numerical Methods for Heat & Fluid Flow*, Vol. 12, No. 6, pp. 637–657.

Roe, P.L., 1981. "Approximatte Riemann solvers, parameter vectors, and difference schemes". *Journal of Computational Physics*, Vol. 43, No. 2, pp. 357–372.

Rumsey, C., 2018. "Turbulence Modeling Resource Web page". `https://turbmodels.larc.nasa.gov/`. URL `https://turbmodels.larc.nasa.gov/`. Last Access: 20-02-2018.

Wilcox, D., 1992. "Dilatation dissipation corrections for advanced turbulence models". *AIAA Journal*, Vol. 30, No. 11, pp. 2639–2646.

8. RESPONSIBILITY NOTICE

The authors are solely responsible for the printed material included in this paper.